Original Manuscript

Journal of Industrial Textiles

Volume 52: 1–16

DOI: 10.1177/15280837221113084
journals.sagepub.com/home/jit
SAGE

Clogging performance of micro/nanofibrous laminated composite air filter media

Mehmet D Calisir[1,2], Melike Gungor[1,3], Ali Toptas[1,4], Utkay Donmez[5], Ali Kilic[1,3] and Semistan Karabuga[5]

Abstract

The performance of fibrous filter media relies on factors such as particle capture efficiency, pressure drop and clogging time. Fiber diameter, porosity and packing density are important web-based factors to improve final filtration performance. In this study, composite nonwoven webs were produced using spunbonded, meltblown and electroblown mats to obtain filter media with different fiber diameter, porosity and packing density. Such a layered composite approach caused huge differences in porosity and packing density, which resulted with improved clogging performance. The average fiber diameter was found to be 65 ± 19.4 nm for electroblown layer (*N*), while that was 1.17 ± 0.38 μm for meltblown (M) and 17.64 ± 2.65 μm for spunbond (S) layers. NM (nanofiber+meltblown) configuration provided 12–13% lower mean flow pore size, which resulted in faster clogging compared to NS (nanofiber + spunbond) mats. The thicker nanofibrous layer resulted in lower pore size and quality factor. Additionally, the composite samples showed a faster-rising pressure drop than the thick microfibrous mats due to smaller pores that clogged quickly. It was also shown that nanofiber coating causes

[1]TEMAG Labs, Faculty of Textile Tech and Design, Istanbul Technical University, Istanbul, Turkey
[2]Faculty of Engineering and Architecture, Recep Tayyip Erdogan University, Rize, Turkey
[3]Areka Group LLC, Istanbul, Turkey
[4]Safranbolu Vocational School, Karabuk University, Karabuk, Turkey
[5]Teknomelt Teknik Mensucat Industry and Trade INC., Kahramanmaras, Turkey

Corresponding author:
Ali Kilic, Istanbul Technical University, TEMAG Lab, Inonu Cad No 65 Gumussuyu, Taksim, Istanbul 34437, Turkey.
Email: alikilic@itu.edu.tr

a linear increase in pressure drop with dust loading, while microfibrous samples exhibited smooth plateau and linear increase after clogging point. Nanofiber layer facilitates cake formation which causes more difficult airflow, and lower dust holding capacity. Among the layered composite mats, the NM configurations were found to be more advantageous due to higher initial filtration efficiency and almost similar dust loading performance.

Keywords
Clogging, air filter, nanofiber, polyamide 6, composite filter

Introduction

Air filtration is one of the basic solutions to provide a cleaner environment by treating polluted air before it is released into the atmosphere. The porous membrane and fibrous filters are the main types of air filter media, while the latter has attracted more interest owing to their larger porosity, flexibility and higher surface area.[1,2] Fibrous filters were typically constructed of matted glass or quartz fibers, woven fabrics of cotton and wool up until 1950s; however, new materials and structures have been employed in this area after the developments in synthetic fibers and nonwoven technologies. Nowadays, the nonwoven fibrous filters can be produced from organic/inorganic and natural/synthetic fibers by several conventional, (i.e. spunbond, air-laid, meltblown etc.,) and novel techniques, (i.e. electrospinning, solution blowing etc.).[3] Fiberglass-based filters, which consist of 1–60 μm glass fibers, have *larger pores* and are the first to come across due to their low cost and high thermal resistance.[4–6] These filters are produced by spun-melt processes in which molten glass is transformed into fibers by passing through perforated nozzles with a constant flow rate, and are able to retain only large particles with low filtration efficiency. However, with the production of microfiber glass filter papers with a diameter of 0.5–1 μm via wet lay process, HEPA (high-efficiency particulate air) filtration via fiberglass media is also possible.[7–9] On the other hand, polymer based nonwoven filters are generally produced by spunbonding or meltblowing techniques. While the diameter of the fibers in spunbond fabrics are in the range of 15–35 μm, melt-blowing generally enables the production of fibers with typically 1–5 μm and in some cases submicron diameter. Meltblown nonwovens have smaller *pores* that provide better filtration efficiency.[10]

There are three main performance assessment criteria of the filters: pressure drop, filtration efficiency and filter lifetime. These properties depend on the structure of filters (packing density, fiber diameter, and thickness), operational conditions (filtration velocity, temperature) and characteristics of the filtered aerosols (density, particle size and distribution). Performance of filter media can be further improved by employing nanofibers that results in increased surface area and lower pressure drop due to slip effect.[11–13] Nanofibrous filters can be produced using different methods, electrospinning,[14] solution blowing,[15] centrifugal spinning,[16] electro-blowing (EB)[17] etc. Among them, EB is an efficient method since both electrostatic and air drag forces are utilized. Shear forces created by high velocity air flowing around the viscous polymer jet and the electrical field

between the collector and blowing nozzle are main driving forces for fiber formation. By combining the electric field forces and the shear forces, it is possible to obtain ultrafine fibers more efficiently via EB technique.

Normally, after a certain period of use, clogging of the filter takes place due to filling of the pores between the fibers with solid particles, which then leads to cake layer formation on the filter surface and causes abrupt increase in pressure drop. It is known that clogging is more likely to occur with filter materials of high packing density and fine fibers. Japuntich et al.[18] reported that the clogging of laminated filter papers was independent of initial filtration efficiency and the amount of the accumulated particles is mainly determined by the filter surface properties. Therefore, fiber diameter, *pore size* and its distribution, surface structure, thickness, applied surface treatment such as anti-fouling, and filtered aerosol particles are some of the important features related to clogging and cleaning kinetics of a filter media.[19,20] Accordingly, a filter with *smaller pores* results in relatively high efficiency but can clog much faster than the filter with *larger pores* that gives lower efficiency. Hence a composite filter media consisting of nanofiber and microfiber layers should be designed carefully as it effects the energy efficiency of the filter media as well as its lifetime.

The majority of the studies in the literature relevant to the clogging performance of filters are on the membranes used in liquid filtration, and according to our best there are few studies in air filtration. Among the studies, Song et al.[21] have investigated the change in pressure drop and filter efficiency in filters during clogging under different parameters e.g. effect of air velocity, particle size, and aerosol concentration parameters. Bourrous et al.[22], on the other hand, examined the effect of ultrafine particles on the pressure drop, filter efficiency and clogging behavior of glass fiber-based HEPA filters and reported a model that allows predicting the clogging profiles of the filters. The model was limited to sub-micron aerosols and to predict the filter lifetime, it used the packing density and thickness of the filter medium, the penetration profile of the aerosols in the medium, as well as the size of the primary particles of the aerosols and the porosity of the deposit. Leung et al.[23] investigated the quality factors of filters made of nanofibers (98 and 300 nm) and microfibers (1.8 μm) and developed an empirical model to determine the distribution of aerosol residue across the filter thickness using experimental data. Accordingly, while the filter surfaces made of nanofibers exhibit high filtration efficiency, they showed high-pressure drop due to the skin effect. They reported that pressure drop can be improved by using a filter surface consisting of microfibers in front of the nanofiber layer.

In this study, the filtration and clogging performances of micro/nanofibrous laminated composite air filters were investigated with respect to various fiber diameters, pore size, and layer configurations. Meltblown and spunbond nonwoven substrates that are widely used on face mask and other filtration applications were employed and PA6 based nanofibrous layers with different thickness were coated via electroblowing in which production rate is 30 times higher than in the conventional electrospinning method.[17] It was also aimed to investigate the response of pressure drop with particle loading and filter clogging, with reference to effective pore diameter. As fiber diameter decreases smaller pores and larged solidity will be obtained at an expense of increased pressure drop and

lower dust holding capacity. At the end of the study, the ideal filter properties were tried to be determined by comparing the clogging results with the filter efficiency.

Experimental

Materials

Polyamide 6 (PA6, from BASF) was dissolved in the mixture of (1:1 wt. ratio) of acetic acid (>99.8% purity, Sigma-Aldrich) and formic acid (>98% purity, Sigma-Aldrich) Three solutions with different concentrations (9, 12, 15 wt.%) were prepared. The spunbond (Teknomelt 2892) and meltblown (Teknomelt 8397) nonwovens were provided from Teknomelt LLC. A sample coding was used as C9E30P3-SB where C stands for concentration, E for the applied electrical field, P for air pressure, and SB for spunbond substrate.

Nanofiber production and laminated composite formation

A lab-scale EB (Aerospinner L1.0, AREKA Group Ltd., Turkey) was used for production of the PA6 based nanofibrous mats on the nonwovens with the help of a vacuum-assisted, rotating collector. A nozzle with 21 gauge needles, an air pressure of 3 bar, a nozzle-to-collector distance of 65 cm, an electrical field of 30 kV, and constant solution feeding rates 30 mL/h were employed for all productions. During the spinning period the measured temperature and relative humidity were 22.3 ± 2°C and 31 ± 2% respectively. Schematic of the electroblowing system was given in Figure 1.

In order to investigate the thickness of the nanofibrous layer on the filtration efficiency and clogging feature of the filter media, the nanofibrous layer was produced at different periods of time, lasting 4, 6, 8 min. Samples were coded with the name of the used substrate and spinning time period similar to MB4*N* for meltblown (MB) nonwoven and 4 min spinning time or SB4N for spunbond (SB) nonwoven and 4 min spinning time. The areal density of nanofiber mats produced after 4, 6 and 8 min was found to be 1, 1.5 and 2 gsm, respectively.

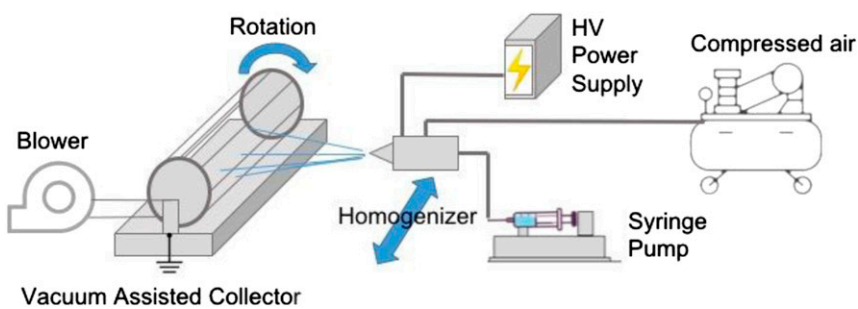

Figure 1. Schematic of the electroblowing system.

Characterization

The viscosity and conductivity of the prepared PA6 solutions were measured using a rotational viscometer (B-One Plus, Lamy Rheology Instruments) and EC Meter (HI-2030 edge Hybrid Multiparameter, Hanna Instruments), respectively. Fiber morphologies were investigated from scanning electron microscope (SEM, Tescan Vega 3) images. Prior to SEM, 10 nm thick gold/palladium layer was sputter-coated on the samples to provide conductivity. Average fiber diameters (AFD) and standard deviations were calculated using 100 measurements obtained from the SEM images at 10 kX magnification. The pore structure of the samples was investigated via capillary flow porometer (Porolux 1000, Porometer) using Galpore 16 wetting fluid with 16 dyn/cm surface tension and nitrogen gas. Filtration performances of the samples were measured with TSI8130 A automated filter testing system. Aerosol particles were produced from 2 wt.% concentration NaCl solution. The average particles size was kept at 0.3 μm, while the flow rate was 95 L/min (face velocity of 15.83 cm/s). Filtration efficiency and pressure drop values were recorded. The QF values were also calculated according to equation (1).[24]

$$QF = -\frac{ln(1-\eta)}{\Delta P} \tag{1}$$

Clogging performance test was performed on NFS Dust Producer system (NFS Engineering Co.). Filter samples with a diameter of 11.5 cm were placed on the sample holder, the lid is closed by a piston and the A1 Ultra Fine Test Dust (quartz particles having size distribution between 1 – 22 μm, PTI Powder Technology INC.) was fed. A1 test powder was transferred at 1 g/min rate till the pressure difference reached 1100 Pa. Then, the filter was weighed to determine the mass collected per unit area.

Results and Discussions

Solution Properties

Viscosity and conductivity values of PA6 solutions prepared at different weight ratios are given in Table 1. Accordingly, as the solution concentration increased, it was observed that both viscosity and conductivity values increased. Additionally, the increase rate of viscosity was higher especially when the concentration value increased from 12 to 15. A similar situation was also seen in the conductivity results. As the

Table 1. The viscosity and conductivity of the prepared solutions.

Solution	Viscosity (mPa.s)	Conductivity (μS/cm)
9 wt.%	176.4 ± 14.8	298.7 ± 2.6
12 wt.%	251 ± 13.8	336.3 ± 1.2
15 wt.%	537.2 ± 29.3	393.6 ± 34

concentration increases, the denser macromolecular ratio in solvents provides minor increase in conductivity.

Morphology of nanofibrous mats

The fiber morphologies were investigated from SEM micrographs (Figure 2) Accordingly, the electroblown nanofibrous mats consist of randomly distributed fibers. It is

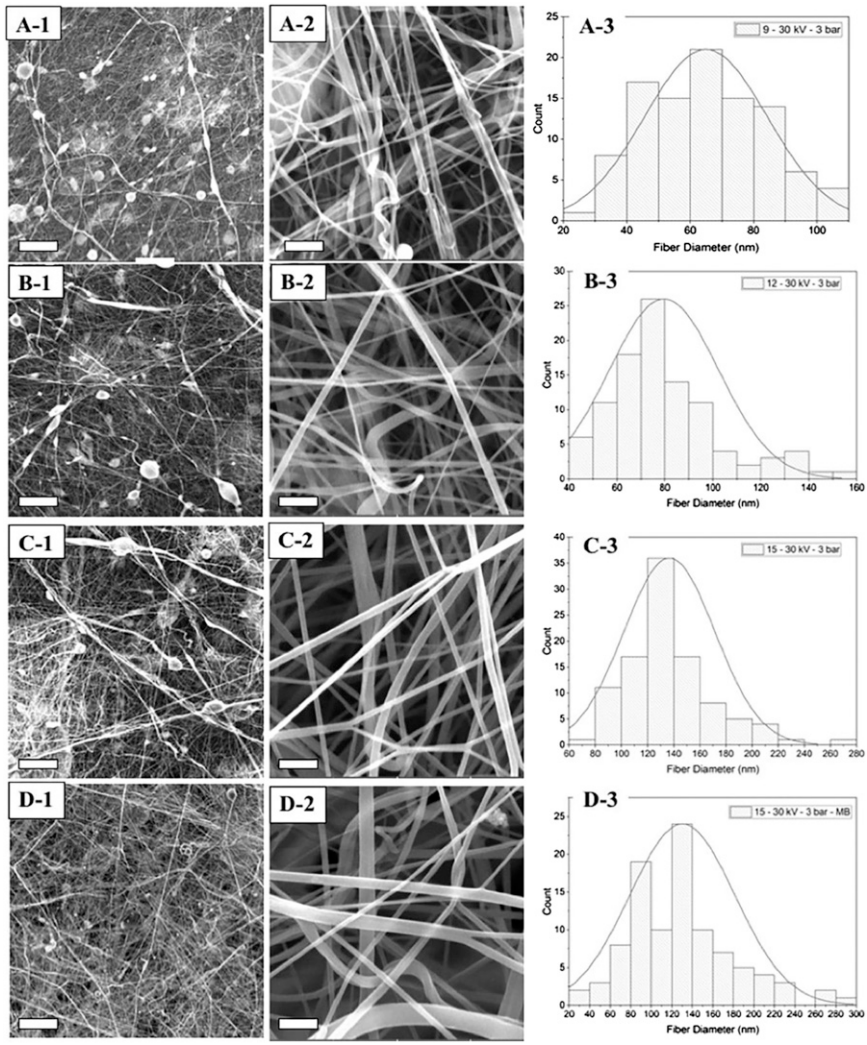

Figure 2. SEM images of a) C9E30P3-SB, b) C12E30P3-SB, c) C15E30P3-SB and d) C15E30P3-MB samples (scale bars are 20 and 1 μm for first and second columns).

observed that the solution concentration had serious effects on the fiber diameter and morphology. In the SEM images with low magnification, a high number of droplets were seen in the PA6 nanofibrous mats produced from the solution with 9 wt.% concentration. Additionally, the amount of the droplets was decreased by increasing solution concentration. Since the insufficient evaporation of the solvent causes droplet formation, the higher amount of droplets in the sample can be attributed to higher solvent content and lower viscosity values of the solution with low concentration. However, increasing PA6 solution concentration up to a certain value (15 wt.%) increases the solution conductivity, as well. Since an increase in solution conductivity and viscosity causes an increase in fiber diameters in the electrospinning method, similar behavior was observed for the electroblown samples.

The AFD values were found as 65.0 ± 19.4 nm, 79.2 ± 22.5 nm and 135.9 ± 33.8 nm for the samples produced from the solutions with 9, 12, 15 wt.% concentrations, respectively. While an increase in the solution concentration resulted in thicker fibers, it lowered the level of dispersion around the mean as seen in the coefficient of the values of the variation in Table 2. Since the thicker fibers negatively affect the particle capture efficiency, samples produced from the 9% solution concentration at which the smallest fiber diameter is obtained were chosen to be used in the rest of the study. On the other hand, change in substrates and their basis weight did not result in an abrupt change in nanofiber diameter. The AFD was found as 132.7 ± 56.3 nm for the sample produced from 15 wt.% PA6 solution on the MB substrate, which was very close to its SB counterpart. However, the CV value was increased which indicated that both the substrate and the vacuum collection has also an effect on the fiber diameter.

Figure 3 shows the SEM images of the MB and SB nonwoven substrates and the their AFD values. While MB nonwoven fabric has finer fibers (1.17 ± 0.38 μm), SB nonwoven fabric has fiber diameters up to 20 μm. According to Figure 2, when the MB nonwoven fabric is used, the bead structure formed in production is less. This can be explained by the fact that the droplets that reached the nonwoven surface encounter more surface area, enhancing the chance to change the morphology from droplet to fiber as a result of the continuous shear force from the pressured air. In addition, the small pore structure of meltblown substrates reduces the vacuum efficiency of the collector. This relatively extends the time of the produced fibers to reach the collector and ensures that the residual solvent in the fiber is evaporated more effectively and thus reduces the number of droplets on the mats.

Table 2. Average fiber diameter, their standard deviation (STD) and coefficient of variation (CV) values.

Samples	AFD (nm)	STD (nm)	CV (%)
9–30 kV–3 bar - SB	65.0	19.4	29.85
12–30 kV–3 bar - SB	79.2	22.5	28.41
15–30 kV–3 bar - SB	135.9	33.8	24.87
15–30 kV–3 bar - MB	132.7	56.3	42.43

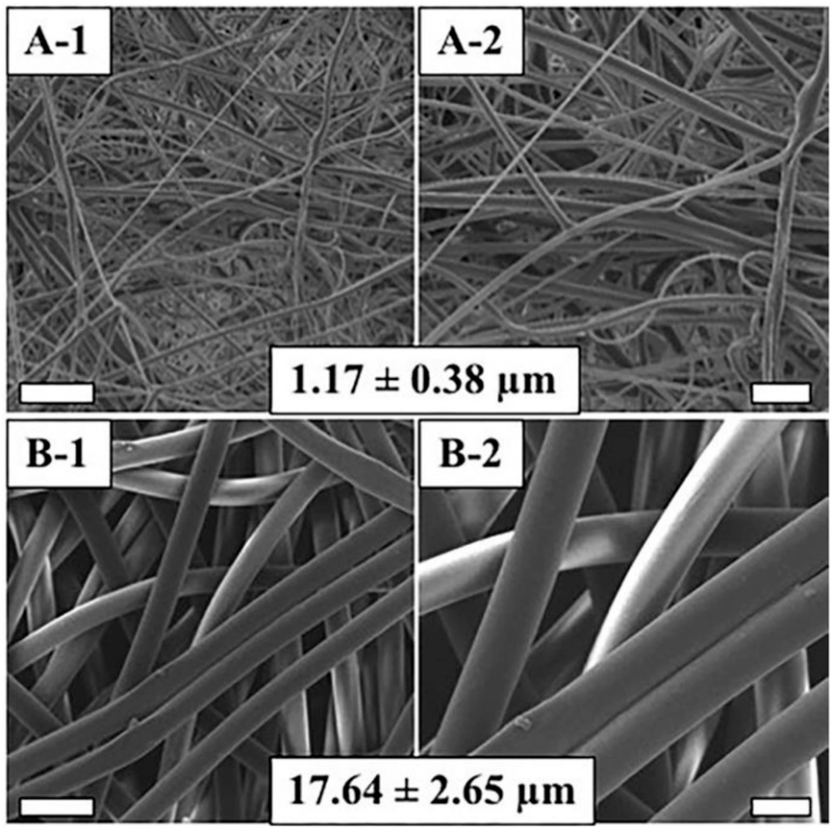

Figure 3. The SEM images of a) MB and b) SB nonwoven substrates at 0.5 (left) and 1 kX (right) magnification (scale bars are 50 and 20 µm for left and right images, respectively).

Pore structure of the composite webs

The mean flow pore (MFP) size of the samples obtained from pressure-flow graphs was given in Figure 4. The lowest MFP size was obtained from MN8 samples which were 30% lower than SN8. Although similar relation was also observed between the MN6 and SN6 samples, the pore size of the MN4 was 10% higher than the SN4. While it is a known fact that meltblown samples have finer pore structures, MN4 sample is expected to have a lower pore size. However, the obtained results were just the opposite and this result can be attributed to thinner nanofibrous mat structure with completely inhomogeneous fiber distribution. Additionally, since the MB substrates have lower pore size and therefore lower air permeability, the efficiency of the vacuum collector is expected to be lower than the obtained in SB. Therefore, the higher pore size might have been explained by obtaining a fluffy nanofibrous layer on the MB substrate, especially for the 4 min production time.

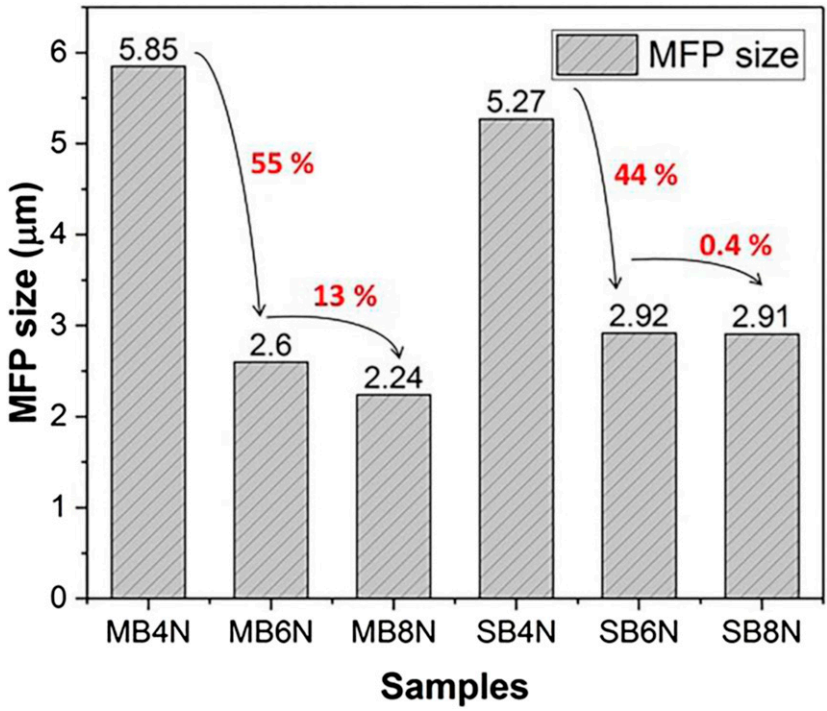

Figure 4. Mean flow pore size distribution of the composite filter media.

The pore size of the samples decreased by 50% due to thicker nanofibrous layer and an increase in thickness resulted in samples with even lower pore size. Similar tendency was obtained from the decrease in average pore size of the samples produced in 6 and 8 min (55% for MN6 and 44% for SN6) than PRR of the samples produced in 8 min (13% for MN8 and 0.4% for SN8). In SN configurations, a more compact nanofiber layer was obtained with a higher vacuum collector effect, which caused the value of the pore sizes to not change much with further increased production time. These results showed that the final pore sizes of the filter samples depend on the thickness of nanofibrous layer and their fiber distribution which was a function of deposition time.

Filtration properties of composite filter media

The filtration performance of all samples was examined and results were given in Figure 5. As expected MB nonwoven exhibited higher filtration efficiency than the SB nonwoven due to its finer fiber structure (~1.2 μm) compared to SB (~17 μm). Although the increase in the deposition time from 4 to 8 min resulted in higher filtration efficiency (from 97.98 to 99.49%), it lowered the quality factor as a result of a larger increase in pressure drop. Moreover, the double-layered MB4N sample exhibited the lowest QF

among the MB-based ones due to higher pressure drop as a result of doubled MB substrate.

On the other hand, nanofiber-coated SB fabrics exhibited lower filtration efficiencies (88.75–95.51%) than their MB-based counterparts. The filtration efficiency was also more affected by the nanofiber depositing time. The maximum filtration efficiency (98.55%), one of the lowest QF (0.0122) values, was obtained from the double-layered SB4N sample due to a larger pressure drop. To summarize all these results, high-quality filters are obtained when MB is used as a substrate in productions made under the same conditions. While filtration efficiency improves with increasing nanofiber thickness in both groups, the double-layered structure resulted in better quality factor only in SB-based ones. This difference is attributed to larger pressure drop difference between SB and MB. The results obtained from the filtration test for each sample were also tabulated in Table 3.

The MFP sizes and quality factors of the produced composite filter samples were compared in Figure 5 and the rate of change that each series showed within itself depending on the nonwoven change was given. The % change in the MFP ratio indicated by

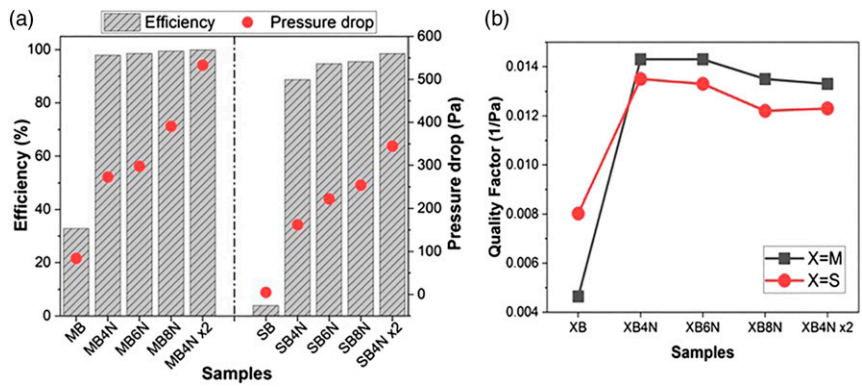

Figure 5. Filtration efficiency, pressure drop and quality factor of the samples.

Table 3. Filtration efficiency, pressure drop and quality factor values of the samples.

Samples	Efficiency (%)	Pressure drop (Pa)	Quality factor (1/Pa)
MB	32.819	84	0.0047
MB4N	97.979	273	0.0143
MB4N x2	99.918	533	0.0133
MB6N	98.581	298	0.0143
MB8N	99.493	391	0.0135
SB	4.005	5	0.0082
SB4N	88.751	162	0.0135
SB4N x2	98.546	345	0.0123
SB6N	94.731	222	0.0133
SB8N	95.507	254	0.0122

the yellow arrows was calculated as 100*(MFPMB4N - MFPSB4N) and the % change in the QF values indicated by the blue arrows was calculated with the formulas 100*(QFMB4N - QFSB4N). In general, it is seen that samples with larger MFP size within the same series show a lower QF value. However, the XB4N series does not comply with this generalization, which can be attributed to the fact that the amount of nanofibers present is not sufficient to form a homogeneous layer on the MB, and the MB fabric with a higher initial pressure drop causes a looser nanofibrous structure by reducing the vacuum effect of the collector. It is seen that the nanofiber production period has a greater effect on the MFP change rate of MB-based samples. The MFP value showed a faster decrease with increasing time, which can be explained by the low surface roughness of MB, which consists of fine fibers, and a smoother nanofibrous layer on top of it. In terms of QF, however, a greater reduction was seen in SB-based samples for the same time periods. The reason for this may be that although the total pore change is less, the amount of nanofibers affects the pressure drop values more in SB-based samples (Figure 6).

Clogging performance

In order to assess the clogging performance, the pressure drop was continuously measured during the particle loading and collected mass during the test period was plotted against the pressure drop in Figure 7. Considering the figures, it is observed that the composite

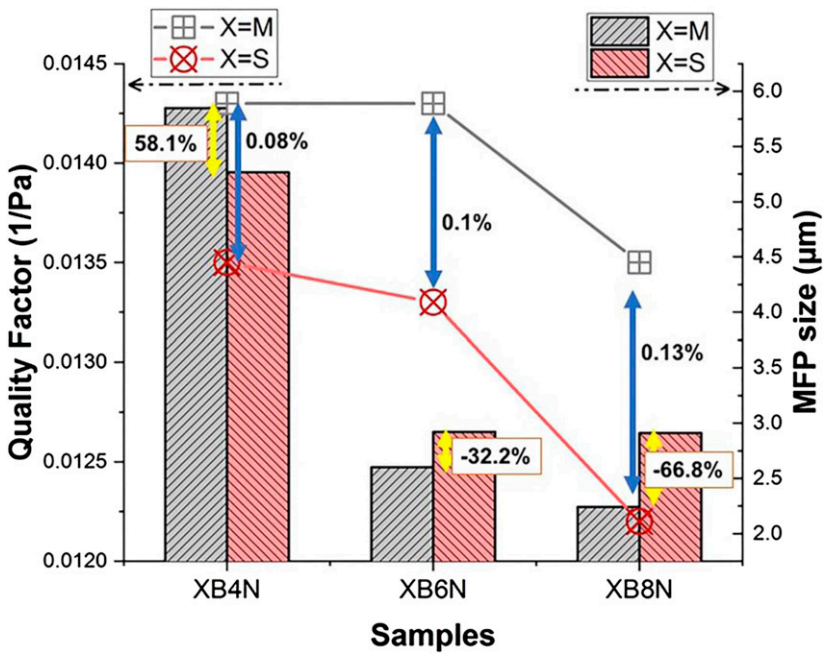

Figure 6. Comparison of the QF and MFP values of the samples.

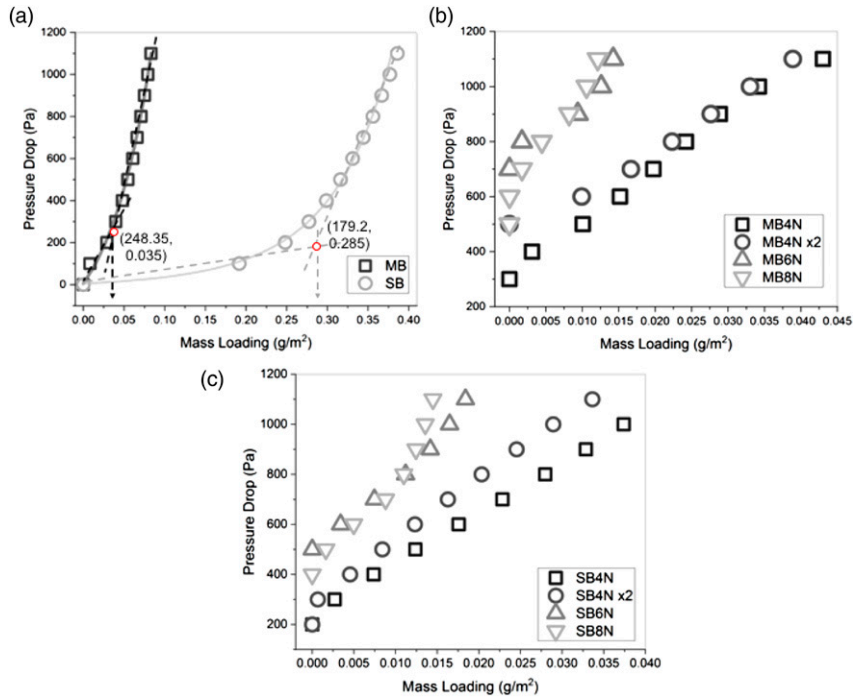

Figure 7. Clogging performance of (a) MB and SB nonwoven fabrics, (b) MB/nanofibrous and (c) SB/nanofibrous composite samples.

samples showed a faster-rising pressure drop than the substrates due to smaller pore sizes that clogged quickly. Therefore, quicker cake formation on the filter surface and subsequently more difficult airflow, and lower dust holding capacity were observed.

In Figure 7(a), the evolution graph of pressure drop during clogging of the substrates was given. The two different slopes were obtained as a common observation for both samples. Among these regimes, the lower one corresponds to depth filtration while the higher one is for surface filtration, and the intersection of the tangents of the two linear portions corresponds to cake formation points.[18] Due to the larger fiber diameter and pore size of the SB fabrics, the cake formation was late, and the depth filtration stage took longer than the MB. The collected mass until the cake formation was nearly 10 times higher for the SB substrate.

According to Figure 7(b), among the MB/nanofibrous samples, the MB4*N* sample showed the maximum mass loadings and it was followed by double-layered MB4*N* with very small differences**.** However, the MB4*N* exhibited a higher pressure drop at the beginning of the test where the loaded mass was very low, which is consistent with the results of the filtration test. An increase in depositing time and therefore thicker nanofibrous layer resulted in quicker cake formation and lower mass loading for the sample MB6N and MB8N. As shown in Figure 7(c), similar results were obtained in the clogging

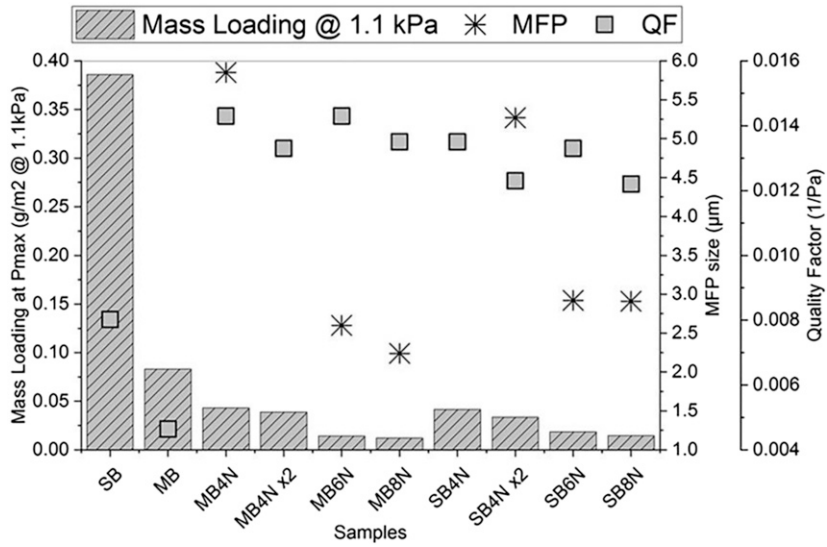

Figure 8. Comparison of clogging, **pore size**, and QF values of all samples.

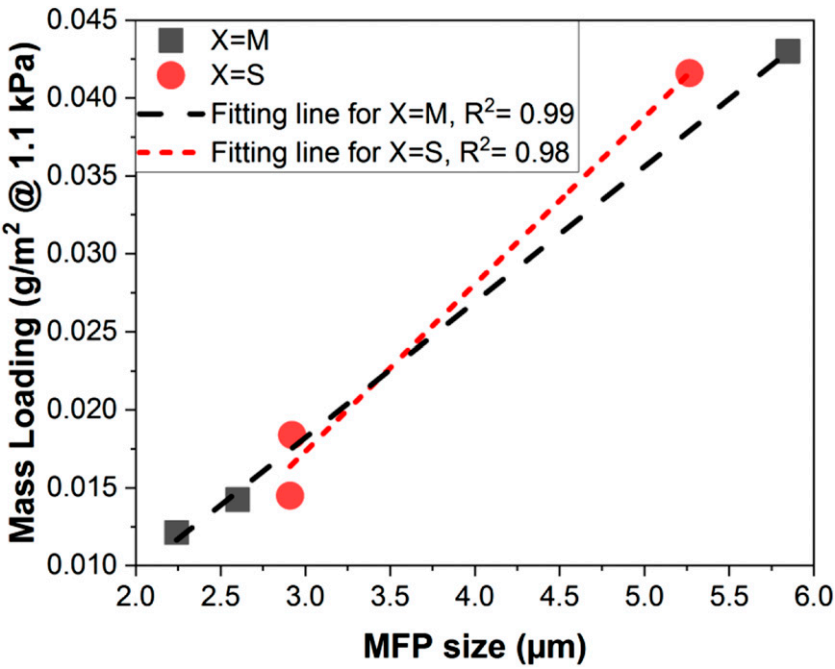

Figure 9. The effect of MFP size on mass loading in clogging tests.

tests performed on SB/nanofibrous composite samples. However, due to SB nonwoven was consisted of larger fibers and thus pores than MB one, the amount of dust holding was higher in SB-based composite filters at an intermediate pressure drop with the help of more effective deep filtration. The reason why the curves with two different slopes could not be obtained in the pressure drop graph as a function of the collected mass in Figures 5(b) and (c) is that the MB and SB/nanofibrous composite filters exhibited quicker cake formation. This is a result of the reduction of the pore size, trapping the particles on the surface of the filter before they can move through the filter.

In Figure 8, clogging, pore size, and QF values of all samples are shown in comparison. As seen in the figure, while the QF is higher in composite samples, they resulted in lower mass loading in the clogging test due to reduced pore size. This situation is more obvious for the samples produced on SB substrates. Although the highest mass loading was obtained from the SB nonwovens, this media can only be used as prefiltration applications due to its lowest efficiency (4%). Additionally, as shown in Figure 9, MFP has an positive relation with mass loading, thus, low MFP resulted in lower mass loading in the composite samples. To sum up, the MB4N will be the best of the choice for the applications that require a higher initial filtration efficiency of >97%, and the maximum mass loading.

Conclusions

The effect of different composite configurations on nano-/microfibrous were investigated from different aspects, ie pore size, submicron particle filtration performance, and dust holding capacity. The PA6 based nanofibrous layers with different thicknesses were produced via the EB technique. Among them the lowest AFD (65.0 ± 19.4 nm) was obtained from the 9 wt.% PA6 solution and the substrate material used did not have a significant effect on the AFD. As the thickness of the nanofibrous layer increased, the pore size of the samples decreased which resulted in these samples being clogged easily and increased pressure drop. The clogging tests showed that cake formation occurred after larger particle loading, and the depth filtration stage took longer in SB than the MB ones due to the larger fiber diameter and pore size of the spunbond fabrics. On the other hand, although the QF was found slightly higher in composite samples, especially in the samples produced on MB substrate, low particle loading was observed due to their reduced pore size. Finally, the MB4N will be the best of the choice for the applications that require a higher initial filtration efficiency of >97%, and the maximum mass loading.

Acknowledgements

The authors gratefully acknowledge AREKA Group LLC (www.arekananofiber.com) and TEKNOMELT LLC for their precious supports.

Declaration of Conflicting Interests

The author(s) declared no potential conflicts of interest with respect to the research, authorship, and/or publication of this article.

Funding

The author(s) disclosed receipt of the following financial support for the research, authorship, and/or publication of this article: This work was supported by The Scientific and Technological Research Council of Turkey (TUBITAK, Grant no 118M035 and TUBITAK, Grant no TEYDEB 7200542).

ORCID iD

Ali Kilic https://orcid.org/0000-0001-5915-8732

References

1. Wang C, Wu S, Jian M, et al. Silk nanofibers as high efficient and lightweight air filter. *Nano Res* 2016; 9: 2590–2597.
2. Stojanovska E, Canbay E, Serife Pampal E, et al. A review on non-electro nanofibre spinning techniques. *RSC Adv* 2016; 6: 83783–83801.
3. Alghoraibi I and Alomari S. Different Methods for Nanofiber Design and Fabrication. In: Barhoum A, Bechelany M and Makhlouf A (eds) *Handbook of Nanofibers*. Cham: Springer International Publishing, 2018, pp. 1–46.
4. Hutten IM. CHAPTER 8 - Air Filter Applications. In: Hutten IM (ed) *Handbook of Nonwoven Filter Media*. Oxford: Butterworth-Heinemann, 2007, pp. 325–367.
5. Shafi S, Navik R, Ding X, et al. Improved heat insulation and mechanical properties of silica aerogel/glass fiber composite by Impregnating silica gel. *J of Non-Crystalline Sol* 2019; 503–504: 78–83.
6. Wang G, Zhang D, Li B, et al. Strong and thermal-resistance glass fiber-reinforced polylactic acid (PLA) composites enabled by heat treatment. *Int J Biol Macromolec* 2019; 129: 448–459.
7. Zhang W, Deng S, Wang Y, et al. Dust loading performance of the PTFE HEPA media and its comparison with the glass fibre HEPA media. *Aerosol Air Qual Res* 2018; 18: 1921–1931.
8. Sparks T and Chase G. Section 3 - Air and Gas Filtration. In: Sparks T and Chase G (eds) *Filters and Filtration Handbook*. 6th edition. Oxford: Butterworth-Heinemann, 2016, pp. 117–198.
9. Hutten IM. Chapter 1 - Introduction to Nonwoven Filter Media. In: Hutten IM (ed). *Handbook of Nonwoven Filter Media*. 2nd edition. Oxford: Butterworth-Heinemann, 2007, pp. 1–52.
10. Hutten IM. CHAPTER 5 - Processes for Nonwoven Filter Media. In: Hutten IM (ed) *Handbook of Nonwoven Filter Media*. Oxford: Butterworth-Heinemann, 2007, pp. 195–244.
11. Choi H-J, Kumita M, Seto T, et al. Effect of slip flow on pressure drop of nanofiber filters. *J Aerosol Sci* 2017; 114: 244–249.
12. Akgul Y, Polat Y, Canbay E, et al. 20 - Nanofibrous composite air filters. In: Jawaid M and Khan MM (eds) *Polymer-based Nanocomposites for Energy and Environmental Applications*. Sawston: Woodhead Publishing, 2018, pp. 553–567.
13. Tang M, Chen S-C, Chang D-Q, et al. Filtration efficiency and loading characteristics of PM2.5 through composite filter media consisting of commercial HVAC electret media and nanofiber layer. *Separat Purif Technol* 2018; 198: 137–145.
14. Lyu C, Zhao P, Xie J, et al. Electrospinning of Nanofibrous Membrane and Its Applications in Air Filtration: A Review. *Nanomaterials* 2021; 11: 1501.

15. Stojanovska E, Ozturk ND, Polat Y, et al. Solution blown polymer/biowaste derived carbon particles nanofibers: An optimization study and energy storage applications. *J of Energ Storage* 2019; 26: 100962.
16. Tepekiran BN, Calisir MD, Polat Y, et al. Centrifugally spun silica (SiO2) nanofibers for high-temperature air filtration. *Aerosol Sci Technol* 2019; 53: 921–932.
17. Gungor M, Toptas A, Calisir MD, et al. Aerosol filtration performance of nanofibrous mats produced via electrically assisted industrial-scale solution blowing. *Polym Eng Sci* 2021; 61: 2557–2566.
18. Japuntich DA, Stenhouse JIT and Liu BYH. Effective pore diameter and monodisperse particle clogging of fibrous filters. *J Aerosol Sci* 1997; 28: 147–158.
19. Xia T and Chen C. Evolution of pressure drop across electrospun nanofiber filters clogged by solid particles and its influence on indoor particulate air pollution control. *J of Hazard Mater* 2021; 402: 123479.
20. Guo Z-Y, Yuan X-S, Geng H-Z, et al. High conductive PPy–CNT surface-modified PES membrane with anti-fouling property. *Appl Nanoscience* 2018; 8: 1597–1606. DOI: 10.1007/s13204-018-0826-5.
21. Song CB, Park HS and Lee KW. Experimental study of filter clogging with monodisperse PSL particles. *Powder Technol* 2006; 163: 152–159.
22. Bourrous S, Bouilloux L, Ouf F-X, et al. Measurement and modeling of pressure drop of HEPA filters clogged with ultrafine particles. *Powder Technol* 2016; 289: 109–117.
23. Leung WW-F and Hung C-H. Skin effect in nanofiber filtration of submicron aerosols. *Separat Purif Technol* 2012; 92: 174–180.
24. Uppal R, Bhat G, Eash C, et al. Meltblown nanofiber media for enhanced quality factor. *Fibers Polym* 2013; 14: 660–668.
25. Aulova A, Bek M, Kossovich L, et al. Needleless electrospinning of PA6 fibers: the effect of solution concentration and electrospinning voltage on fiber diameter. *Strojniški vestnik – J Mech Eng* 2021; 66: 421–430.
26. Maze B, Vahedi Tafreshi H, Wang Q, et al. A simulation of unsteady-state filtration via nanofiber media at reduced operating pressures. *J Aerosol Sci* 2007; 38: 550–571.